

Experimental Verification of Predicted Sources of G/T Improvement for the DSS-13 Beam-Waveguide Antenna

T. Y. Otoshi,¹ W. Veruttipong,¹ J. Sosnowski,¹ and R. Cirillo, Jr.¹

This article presents the results of tests performed to verify predicted sources of receive antenna gain-to-system noise temperature ratio (G/T) improvements for the DSS-13 beam-waveguide antenna. The sources that gave the most improvement were (1) covering holography adjustment holes with aluminum-tape circular disks, (2) covering all panel gaps on the main-reflector surface with aluminum tape, and (3) installing a liquid-nitrogen load to capture stray signals that normally would be absorbed by an ambient environment. The total measured improvement for all sources of improvement tested was 1.2 K at 8.420 GHz and 2.9 K at 32 GHz. The improvement was larger at 32 GHz because a liquid-nitrogen load test was not performed at 8.420 GHz.

I. Introduction

The Deep Space Network (DSN) consists of an array of large antennas located worldwide for deep-space communication. Improving the G/T of these antennas and their associated receive subsystems translates into increasing the ground received-signal-to-noise ratios. The symbol G refers to the receive antenna gain and T refers to the system noise temperature. The primary objectives of the G/T improvement task are to (1) identify sources where G/T improvements can be made and (2) verify the predicted values through analysis or experimental work.

For convenience, in this article the terms system temperature and operating system temperature, T_{op} , will be used interchangeably to mean system-noise temperature, and the terms S-, X- and Ka-band will be used to refer to center frequencies of 2.295, 8.420, and 32 GHz, respectively. Although the goal is to simultaneously improve both G and T , the experimental work was restricted to testing only improvements of system temperature. Any receive-system gain changes caused by a change in test configuration are assumed to be negligibly small or to be predictable through theoretical calculations.

The sources of improvement and predicted improvement values at X- and Ka-band are shown in Table 1. Some of the values were derived from theoretical predictions while others were based on previous experimental work on the DSS-13 beam-waveguide (BWG) antenna [1]. Even though most of the

¹ Communications Ground Systems Section.

The research described in this publication was carried out by the Jet Propulsion Laboratory, California Institute of Technology, under a contract with the National Aeronautics and Space Administration.

Table 1. Suggested G/T improvements for 34-m BWG antennas with predicted improvements and estimated cost.^a

Item	Suggestions for G/T improvements	Predicted X-/Ka-band improvement at 90-deg elevation angle	Estimated cost, \$k
1 ^b	Assemble skirts behind the subreflector.	0.1–0.3 K	12
2 ^b	Cover hatch door opening.	0.03 K	Negligible
3 ^b	Cover openings at base of struts.	0.1–0.2 K	15
4 ^b	Cover holography holes.	0.2–0.4 K	10
5 ^b	Close panel gaps.	0.2–0.3 K	10
6	Readjust panel using holography.	0.18 dB at Ka-band	25
7	Eliminate perforations using a solid panel.	0.2 K at X-band 0.4–0.7 K at Ka-band	Very high
8 ^b	Reduce the size of BWG opening hole near fl.	0.1–0.2 K	10
9	Close the gaps between mirrors and shroud.	0.1–0.3 K	10
10	Add skirt around the horn aperture.	0.1–0.2 K	10
11	Fabricate a new plug at the center of M5.	0.2–0.3 K	10
12 ^b	Install a flat cryo load behind a dichroic plate.	0.5–1.0 K	30

^aThis table was taken from W. Veruttipong and T. Otoshi, *TMO Technology Program Mid-Year Review*, (internal document), Jet Propulsion Laboratory, Pasadena, California, April 1, 1998. Items 2 through 5 are subdivisions of former Items 2 and 3.

^bExperimental verification tests were performed, and the results are reported in this article.

individual improvement values are small (less than 0.4 K), the sum of all improvement values adds up to a significant amount (2 to 4 K) at Ka-band.

Due to manpower and budget constraints, only those experimental tasks that could be done in a reasonable length of time at low cost were selected. Sources of noise-temperature improvement that were tested were (1) covering undesired openings on the dish surface with aluminum tape, (2) covering holography adjustment holes with aluminum-tape circular disks, (3) reducing the normal BWG opening at the dish surface, (4) installing a cone transition to reduce the BWG opening more gradually to a smaller opening at the dish surface, (5) installing subreflector skirts, (6) installing a liquid-nitrogen load to capture stray signals that normally would be absorbed by an ambient environment, and (7) covering all panel gaps on the main-reflector surface with aluminum tape.

In Section II, details are given of the test configurations and tests results. Section III will give recommendations on the G/T improvement configurations that should be implemented.

II. Test Configurations and Test Results

Verification tests were performed on seven different G/T improvement configurations. Descriptions of the test configurations and results of the tests that were performed are presented below in chronological order.

A. Covered Openings on Hatch Door and Tripod Leg Bases

The first of the series of G/T improvement tests involved covering an opening 30.5 cm by 30.5 cm (12 in by 12 in.) on the hatch door with aluminum tape. This opening served as a porthole through

which a person could view the dish surface from below the surface without having to open the hatch door. Aluminum tape was used to cover this hatch door opening (Fig. 1) as well as to cover the openings at bases of the tripod legs (Fig. 2). The function of the aluminum tape on the dish surface was to reflect incoming signals back to the sky rather than allow them to pass through the openings and be absorbed by the ground environment.

The test results in Table 2 show that taping the openings caused the system temperature to be lowered by 0.08 K at X-band and 0.24 K at Ka-band. The measured improvements and predicted values (see Table 1, Item 3) are in good agreement. However, it should be pointed out that, prior to the test, the base of one of the tripod legs was already covered with aluminum tape and the aluminum tape on the base of another leg was partially peeling off. This implies that improvements would have been larger had aluminum tape not already covered the openings at the bases of two of the tripod legs.

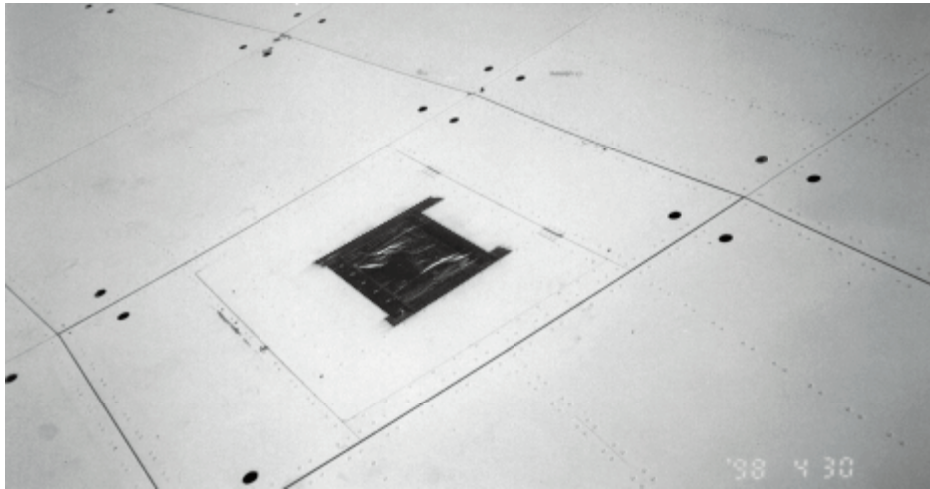


Fig. 1. Aluminum tape covering the opening on the hatch door.



Fig. 2. Aluminum tape covering the base of a tripod leg.

Table 2. System temperatures before and after taping openings on hatch door and tripod bases.^a

Test configuration	8.420-GHz T_{op} , K	32-GHz T_{op} , K	Comments
Before taping	43.74 ± 0.05 $N = 105$	73.48 ± 0.04 $N = 105$	—
After taping	43.66 ± 0.02 $N = 370$	73.24 ± 0.08 $N = 370$	—
Change	-0.08 ± 0.05	-0.24 ± 0.09	Minus-sign change means improvement.

^a T_{op} values are the result of averaging measured T_{op} values over the test period and include corrections for weather. Tolerances include standard deviations due to measurement scatter. N is the number of points used in the averaging and, unless otherwise specified, the integration time for each point was 6 s. Total test period is equal to $N \times 6$ s.

B. Covered Holography Holes

On all DSN antennas, small holes on the dish surface are purposely left uncovered to allow easy access to bolts that lay below the dish surface and are used for panel height adjustments based on holography-measurement results. These holes will be referred to as holography holes. There are 1714 holography holes on the BWG antenna dish surface. Each hole has a diameter of 3.18 cm (1.25 in.). Predicted values in Table 1 show that about a 0.2- to 0.4-K lowering of system-noise temperature can be achieved if the holography holes were to be covered with aluminum tape.

To verify these predictions, circular aluminum-tape disks, each having a 4.32-cm (1.7-in.) diameter, were made and individually placed on 5.08-cm- (2-in.)-wide rolls of waxed paper (see Fig. 3). Each of these disks can be easily peeled off the waxed-paper roll whenever needed. The term “dot” will be used to describe one of these aluminum disks. On November 19, 1998, dots were used to cover all 1714 holography holes on the DSS-13 BWG dish surface. Figure 4 shows dots that were taped over two holography holes on adjacent antenna panels. System-temperature measurements, made before and after the dots were taped over all holography holes, showed that the final system temperature was lowered by 0.35 ± 0.05 K for X-band, which is within the range of 0.2- to 0.4-K predicted values shown in Table 1.

The same experiment was performed by M. Franco of JPL on the DSS-26 BWG antenna using a different radiometer for his measurements. His measured result for 8.420 GHz was 0.3 ± 0.05 K, which agrees well with the X-band result obtained at DSS 13.

The tests were repeated again on December 10, 1998, specifically to measure only the improvement at Ka-band. However, since the DSS-13 dual-radiometer system can measure system temperatures on two different systems (S-/X-band or X-/Ka-band) simultaneously, system temperatures were measured at both X- and Ka-band. As a result of the previous November 19, 1998, test, dots already covered all holography holes on the DSS-13 BWG antenna. It was desirable to have all holography holes covered at the end of this new test. Therefore, the test procedure was altered. The procedure used was first to measure system temperature with dots covering all holes to establish a baseline. Then system temperature again was measured after removing only half the number of dots. A final set of system-temperature measurements was made after covering all holes with dots again. It was found that removing half the dots caused an increase of system-noise temperature of 0.18 ± 0.05 K at 8.420 GHz and 0.25 ± 0.08 K at 32 GHz. These values were determined after correcting system temperatures for (1) receiver gain changes, (2) atmospheric noise temperature changes, and (3) system drift that occurred during the measurements.

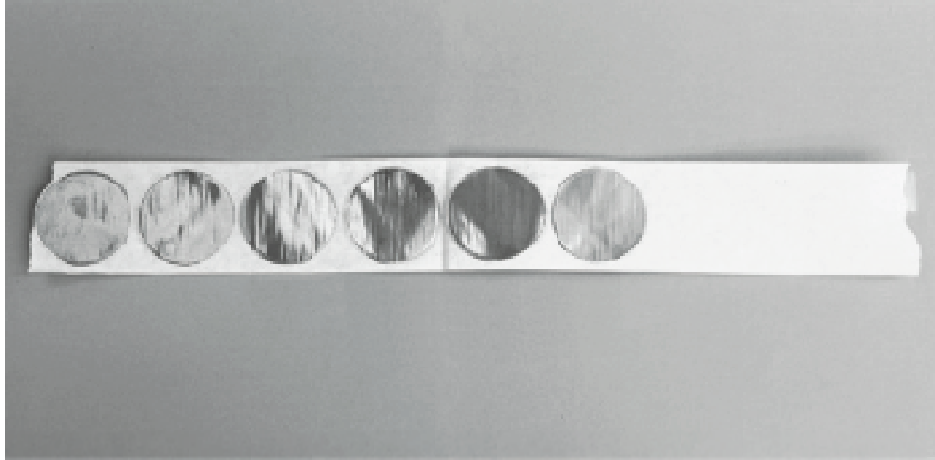


Fig. 3. Aluminum dots on a strip of waxed paper.

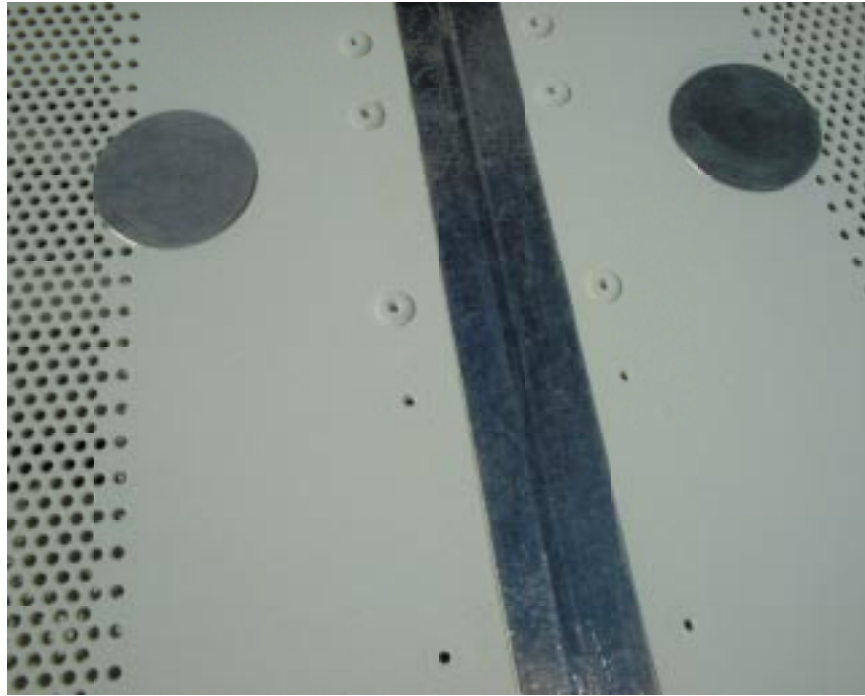


Fig. 4. Aluminum dots covering two of the holography holes on adjacent main-reflector panels.

If the above results are extrapolated to the case when all the dots are removed, then it is reasonable to expect the noise temperature increase to be doubled. Conversely, it then is reasonable to state that covering all holes versus covering no holes would have resulted in a lowering of system temperature of 0.36 ± 0.10 K at 8.420 GHz and 0.50 ± 0.16 K at 32 GHz. This extrapolated value of 0.36 ± 0.10 K agrees well with the 0.35 ± 0.05 K result for 8.420 GHz obtained on November 19, 1998.

C. Reduced BWG Opening

1. Aperture Plate Mounted on Cassegrain Cone Flange. Another G/T improvement test involved reduction of the nominal BWG hole diameter of 2.438 m (96 in.) at the dish surface with an aperture plate (see Fig. 5). For a properly designed BWG system, most of the power from the far field will

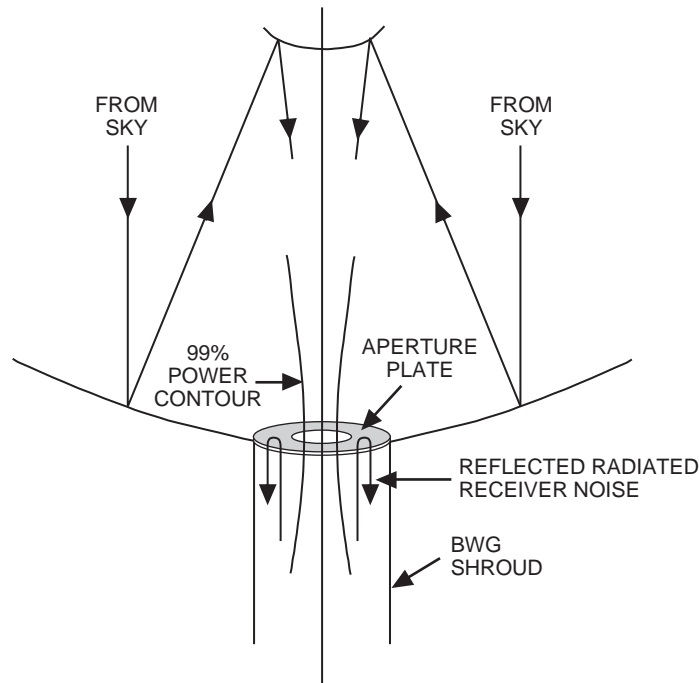


Fig. 5. Radiated receiver noise being reflected by the aperture plate.

reflect off the subreflector and enter the BWG hole within the 99 percent beam contour. However, about 1 percent of the power will stray outside this contour, and some of this stray power that enters the BWG hole will be absorbed by the shroud walls or be absorbed inside the BWG system at ambient temperature. This absorption at ambient temperature causes system temperature to rise. Therefore, it seems reasonable that, if the BWG opening is made smaller to allow only the power within the 99 percent beam contour to enter the BWG system and to reflect the remainder back to the sky, then system temperature would decrease. However, an opening too small will cause more of the radiated receiver-noise temperature [2] to be blocked by the plate so that, instead of allowing it to radiate out the opening to cold sky, it causes more of the radiated receiver power to reflect back towards the receiver. This reflected radiated receiver temperature will pick up additional wall-loss contributions and finally combines with the effective receiver noise temperature to cause the system temperature to increase. In the limit, if the hole diameter were made zero so that all of the radiated receiver temperature were reflected, the system-temperature increase would be about 300 K. This phenomenon was observed in earlier experiments performed in 1991.

The experiments performed to test the BWG hole-reduction theory involved the fabrication of an aperture plate (a plate with a hole in the center). The outer diameter of the aperture plate was designed to be the same as the outer diameter of the Cassegrain cone mounting flange that is located slightly below the surface of the dish. The aperture plate then could be placed on top of the Cassegrain cone mounting flange for support purposes.

Commercially available foam sheets about 3.56-cm (1.4-in.) thick, with aluminum foil glued to both surfaces, were used to make the aperture plate. A 3.048-m (10-ft) outer-diameter disk was first cut with a razor blade, and then annular removable rings of various inner diameters were cut into this sheet but not removed (see Fig. 6). After installation on the Cassegrain mounting flange, by removing the inner rings in a systematic sequence, the aperture plate opening could be easily changed from diameters of 0.61 m (2 ft) to 1.83 m (6 ft) in 0.305-m (1-ft) steps. Figure 7 shows one of these annular rings removed from the fabricated aperture plate.

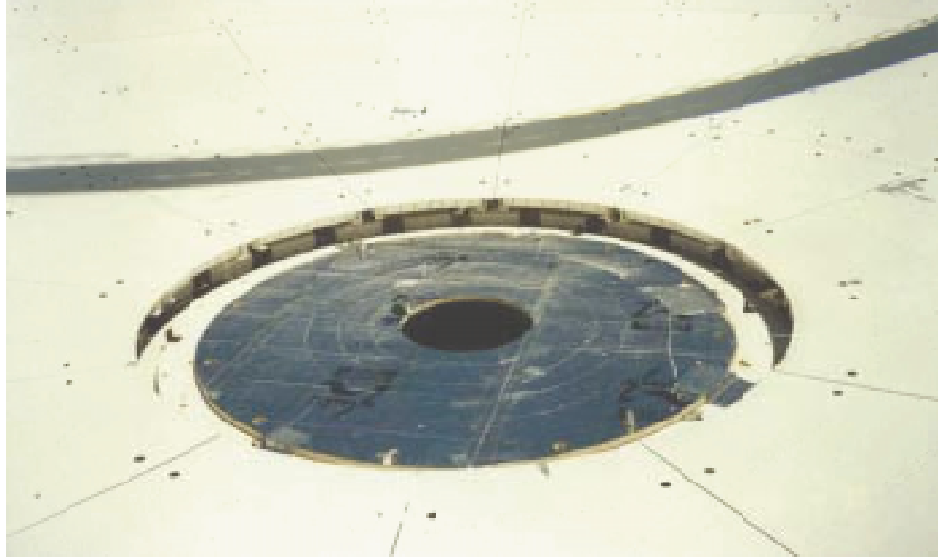


Fig. 6. Aperture plate with a 0.61-m- (2-ft)-diameter hole opening installed on the dish surface of the DSS-13 BWG antenna.



Fig. 7. Aperture plate shown with one of the annular rings removed.

In May 1998, the aperture-plate tests were conducted. The test plan was to determine the optimum BWG opening diameter that will maximize improving system temperatures at both X- and Ka-band with acceptable degradation at S-band. System-temperature measurements first were made with the aperture plate removed. System temperatures subsequently measured for various hole-opening diameters were compared with the system temperature measured with the aperture plate removed. Results of these tests are shown in Table 3. A maximum lowering of system temperature of 0.65 K was observed at 8.420 GHz when the hole diameter was 0.91 m (3 ft). A maximum lowering of system temperature of 0.3 K was

Table 3. Noise-temperature change versus aperture-plate hole diameter.^{a,b}

Hole diameter, m (ft)	Noise-temperature change, K			Comments
	2.295 GHz	8.420 GHz	32 GHz	
0.61 (2)	84.35 ± 0.15 $N = 53$	0.15 ± 0.02 $N = 53$	0.13 ± 0.06 $N = 53$	Degradations at all frequencies.
0.91 (3)	34.40 ± 0.16 $N = 53$	-0.65 ± 0.01 $N = 62$	-0.08 ± 0.09 $N = 62$	Improvements at 8.420 and 32 GHz.
1.22 (4)	11.99 ± 0.19 $N = 53$	-0.57 ± 0.02 $N = 53$	-0.21 ± 0.09 $N = 53$	Improvements at 8.420 and 32 GHz.
1.52 (5)	3.25 ± 0.43 $N = 52$	-0.39 ± 0.03 $N = 55$	-0.29 ± 0.10 $N = 55$	Improvements at 8.420 and 32 GHz.
1.83 (6)	2.11 ± 0.34 $N = 51$	-0.26 ± 0.27 $N = 51$	Did not measure.	Cloudy weather during 32-GHz test. No data taken.

^aThe noise-temperature changes are derived from subtracting the system temperature of the normal BWG 2.438-m (8-ft) hole-diameter configuration from the measured system temperatures of the aperture-plate configurations. Plus-sign noise temperature means degradation. Minus-sign means improvement.

^bNoise-temperature values are the result of averaging measured T_{op} values over the test period and include corrections for weather and baseline drift due to gain changes. Tolerances include standard deviations due to measurement scatter and uncertainties in baseline corrections for drift. N is the number of points used in the averaging and, unless otherwise specified, the integration time for each point was 6 s. The total test period is equal to $N \times 6$ s.

observed at 32 GHz when the hole diameter was 1.52 m (5 ft). At 2.295 GHz, degradations were observed for all of the reduced diameters, and the degradation was as much as 84.4 K when the hole diameter was 0.61 m (2 ft).

2. Aperture Plate Mounted Above the Dish Surface. A more thorough analysis indicated that the narrowest-beam waist lay in a region above the Cassegrain cone mounting flange. Therefore, it was of interest to perform the same tests with the aperture plate raised above the dish surface. This was accomplished by installing four vertical steel rods on the Cassegrain cone-mounting flange (see Fig. 8). The steel rods had threaded portions that allowed the aperture-plate assembly to be raised between 30.48 cm (1 ft) and 152.4 cm (5 ft) above the Cassegrain cone mounting flange.

After installation of the raised aperture-plate assembly to a height of 1.22 m (4 ft), system-temperature measurements were made for various aperture-plate hole openings. Table 4 shows that, when the aperture plate was raised 1.22 m (4 ft), some differences (>0.2 K) of system temperatures were observed from those shown in Table 3 for the same hole diameters. However, Table 5 shows that, when the aperture plate was raised only 38.1 cm (15 in.), the measured improvement was 0.43 K at 32 GHz when the hole diameter was 1.83 m (6 ft). This measured improvement is significantly greater than the 0.08-K improvement value that was measured when the aperture plate (with the same 1.83-m hole diameter) was mounted 1.22 m (4 ft) above the Cassegrain cone mounting flange (see Table 4). The 0.08-K value in Table 4 is thought to be an experimental error due to inability to correct for changing cloudy weather conditions.

During some of these tests, clouds overhead made it difficult to obtain more reliable and conclusive test data at Ka-band. Weather corrections can be made for clear-sky conditions but could be invalid when the sky has moving clouds. It was felt that it was important to report these results rather than to discard them. These Ka-band results might be useful for comparison purposes if tests are redone in the future under clear-sky conditions. The X-band results, however, are not as sensitive to overcast, cloudy conditions, and hence are believed to be valid.



Fig. 8. Aperture plate mounted 1.22 m (48 in.) above the Cassegrain cone mounting flange.

Table 4. Noise-temperature change versus hole diameter when the aperture plate was mounted 1.22 m (48 in.) above the Cassegrain cone flange plane.^{a,b}

Hole diameter, m (ft)	Noise-temperature change, K			Comments
	2.295 GHz	8.420 GHz	32 GHz	
0.91 (3)	Did not test.	-0.21 ± 0.02 $N = 54$	-0.05 ± 0.05 $N = 54$	Some improvement at 8.420 GHz, but small improvement at 32 GHz.
1.22 (4)	Did not test.	-0.33 ± 0.03 $N = 52$	-0.53 ± 0.05 $N = 52$	Large improvement at 32 GHz.
1.52 (5)	Did not test.	-0.33 ± 0.02 $N = 56$	-0.44 ± 0.06 $N = 56$	Improvements at both 8.420 and 32 GHz.
1.83 (6)	Did not test.	-0.31 ± 0.03 $N = 51$	-0.08 ± 0.05 $N = 51$	Results at 32 GHz are thought to be erroneous.

^a The noise-temperature changes are derived from subtracting the system temperature of the normal BWG 2.438-m (8-ft) hole-diameter configuration from the measured system temperatures of the aperture-plate configurations. Plus-sign noise temperature means degradation. Minus-sign means improvement.

^b Noise-temperature values are the result of averaging measured T_{op} values over the test period and include corrections for weather and baseline drift due to gain changes. Tolerances include standard deviations due to measurement scatter and uncertainties in baseline corrections for drift. N is the number of points used in the averaging and, unless otherwise specified, the integration time for each point was 11 s. The total test period is equal to $N \times 11$ s.

D. Tapered BWG Hole Opening

Based on the aperture-plate test results, it was concluded that, if the BWG opening at the Cassegrain mounting flange could be reduced to a smaller diameter by means of a linearly tapered transition (see Fig. 9), the radiated receiver-noise temperature would be guided smoothly out the BWG opening and go to cold sky. Then system temperature should be reduced both by the reduced hole opening and the

smooth transition. To implement this supposition into practice, a cone transition was fabricated from 3.56-cm- (1.4-in.)-thick Styrofoam sheets covered with aluminum foil on both surfaces. Figures 10 and 11 show this fabricated cone assembly being prepared for insertion into the BWG opening at the dish surface. The inside diameter at the bottom of the cone is about 2.44 m (8 ft) so that, when inserted into the BWG opening, the circumferential outside surfaces at the bottom of the cone will touch the BWG shroud wall. The cone is linearly tapered towards the top end to an inside diameter of 1.52 m (5 ft) and has an overall length of about 3.35 m (11 ft). Upon insertion of the cone assembly into the BWG opening, the large mounting flange, shown in Figs. 10 and 11, rests on top of the Cassegrain cone mounting flange.

Table 5. Noise-temperature change versus hole diameter when the aperture plate was mounted 38.1 cm (15 in.) above the Cassegrain cone flange plane.^{a,b}

Hole diameter, m (ft)	Noise-temperature change, K			Comments
	2.295 GHz	8.420 GHz	32 GHz	
1.52 (5)	Did not test.	-0.28 ± 0.03 $N = 47$	-0.35 ± 0.13 $N = 47$	Improvements at both 8.420 and 32 GHz.
1.83 (6)	Did not test.	-0.28 ± 0.03 $N = 50$	-0.43 ± 0.05 $N = 50$	Improvements at both 8.420 and 32 GHz.

^aThe noise-temperature changes are derived from subtracting the system temperature of the normal BWG 2.438-m (8-ft) hole-diameter configuration from the measured system temperatures of the aperture-plate configurations. Plus-sign noise temperature means degradation. Minus-sign means improvement.

^bNoise-temperature values are the result of averaging measured T_{op} values over the test period and include corrections for weather and baseline drift due to gain changes. Tolerances include standard deviations due to measurement scatter and uncertainties in baseline corrections for drift. N is the number of points used in the averaging and, unless otherwise specified, the integration time for each point was 6 s. The total test period is equal to $N \times 6$ s.

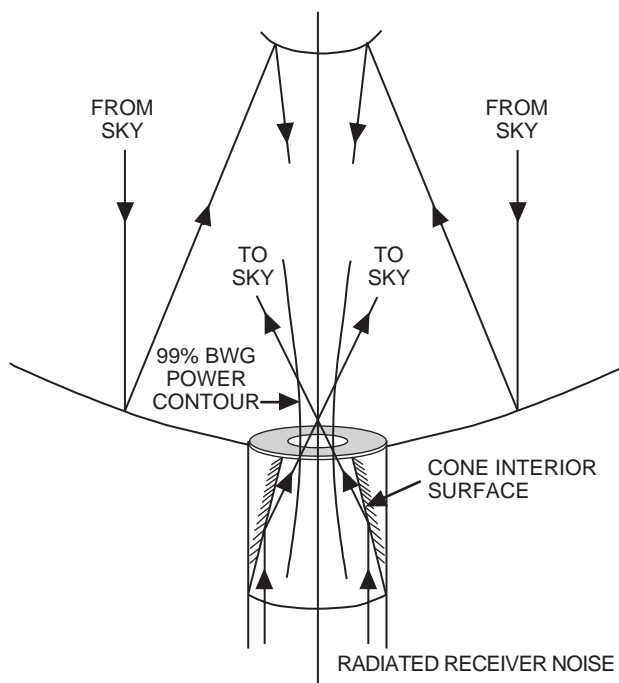


Fig. 9. A cone transition for guiding the radiated receiver noise out the hole opening to the sky.



Fig. 10. Exterior view of the fabricated cone-transition assembly being tilted for installation into the normal 2.44-m (8-ft) BWG opening on the dish surface.



Fig. 11. Interior view of the cone-transition assembly. The cone has a 1.52-m- (5-ft)-diameter opening on the near end and a 2.44-m- (8-ft)-diameter opening on the opposite end.

To verify that the aluminum-foil-covered Styrofoam sheet was a good conductor, measurements of the return losses on a sample of this sheet were made over a frequency range of 32 to 34 GHz. The measured return loss at 32 GHz was about 0.02 dB for either aluminum face as compared with a measured return loss of 0.003 dB for a flat brass-plate short. If 100 percent of the power were incident on the aluminum-foil surfaces, then the noise-temperature contribution would be 1.3 K. However, if instead the power incident on the surfaces were a maximum of 1 percent, as it would be in the test configuration of Fig. 9, then the maximum noise-temperature contribution due to the cone transition would be only 0.013 K.

On January 28, 1999, system-temperature measurements were made at S-, X-, and Ka-band both before and after installation of the cone transition. For the data processing, the first step was to make corrections for the effects of weather on atmospheric noise temperature, T_{atm} , using ground-level weather data and an atmospheric layer model. The program used to make these weather corrections was written by S. Slobin of JPL and modified by T. Otoshi [3]. After correcting for atmospheric noise-temperature changes, the second step in the data-reduction process was to make corrections for baseline drifts.

The corrected test results are shown in Table 6. Comparison with the 1.52-m (5-ft) hole-diameter results of Table 3 shows that the cone-transition results were poorer than the aperture-plate results with the 1.52-m opening. A reason why measured improvements in Table 6 were poorer might be inadequate corrections made for changing cloudy conditions and large baseline drifts. The atmospheric noise temperature corrections, using ground surface weather data, are valid only for clear-sky conditions. The total length of time going from baseline (normal) configuration to the inserted cone-transition test configuration and back to the baseline configuration was about 4 to 6 hours. The baseline drifts were 0.21, 0.20, and 0.74 K at 2.295, 8.425, and 32 GHz, respectively. The baseline drift at 32 GHz was notably large.

It is recommended that these cone-transition tests be redone in clear weather in the future, using improved test procedures that were developed later and will be described in Section II.G of this article.

**Table 6. Cone-transition test results.
(Top of cone has a 1.52-m (5-ft) opening.)**

Frequency, GHz	Change in system temperature, ^a K	Comments
2.295	1.34 ± 0.02	Degradation.
8.420	-0.08 ± 0.04	Improvement.
32.0	0.01 ± 0.07	Degradation or improvement if negative tolerance is applied.

^aThe tolerances shown are uncertainties due to measurement standard deviations and uncertainties in the corrections for atmospheric noise temperature changes and baseline drifts.

E. Subreflector Skirts

On February 11, 1999, noise-temperature tests were performed covering portions of the subreflector edge regions with five reflector plates. A plate was installed near the top of each tripod leg. This test configuration will be referred to as the three-plate subreflector skirt configuration. Two additional plates were installed later to cover the subreflector control structure.

Normally, without these installed reflector plates, small amounts of subreflector spillover power are scattered towards the ground, thus raising system temperature. The installed plates are designed to reflect that portion of subreflector spillover power towards the main reflector, which re-reflects it to the

sky. The lowering of noise temperature due to the installed plates was expected to be between 0.1 and 0.3 K at both X- and Ka-band (see Item 1 of Table 1).

Experimental verification tests showed that the three-plate subreflector skirt configuration caused a lowering of the system temperatures of 0.09 ± 0.05 K at 8.420 GHz and 0.13 ± 0.06 K at 32 GHz. Adding two additional plates to cover the subreflector control structure did not improve the three-plate results at either 8.420 or 32 GHz. The measured improvements are within the 0.1- to 0.3-K range of values that was predicted.

It took about 1 to 1.5 hours to change skirt test configurations. During these configuration changes, radiometer system drifts of about 0.1 K/h were observed on Ka-band measurements. Even after making corrections for atmospheric noise-temperature changes and baseline drift, uncertainties of about ± 0.05 K still existed in the test results. These uncertainties are believed to be as small as can be achieved when using the described correction methods for weather and baseline drifts. It is suggested that, at some future date, these subreflector skirt experiments be repeated when the sky is clear, using the new test procedure that will be described in Section II.G.

F. Liquid-Nitrogen Load

A liquid-nitrogen (LN) load in a Styrofoam bucket was designed to be placed behind and above the X-/Ka-band dichroic plate in the DSS-13 BWG system. Without the LN load, stray Ka-band signals that do not pass through the X-/Ka-band dichroic plate will reflect up to the ceiling, which is at a physical temperature of 300 K. With the LN load installed, these reflected signals will instead be absorbed by the LN load, which is at a physical temperature of about 80 K. Depending on the percentage of power that is reflected toward the LN load, a significant lowering of system temperature can result at Ka-band. The LN load that was developed by the authors for this purpose is shown in Fig. 12. The pyramidal absorbers are installed face down inside a rectangular foam container that has inside-area dimensions of



Fig. 12. JPL-developed Ka-band liquid-nitrogen load. An absorber piece was removed and shown in an upright position for purposes of this picture. The interior was lined with a Kapton sheet to keep liquid nitrogen from leaking out of the foam container.

38.1 cm (15 in.) by 43.18 cm (17 in.). When ready for use, liquid nitrogen is poured into this container. An exterior view of this load assembly installed at DSS 13 is shown in Fig. 13. For convenience, this particular LN load will be referred to as the JPL LN load.

On August 10, 1999, tests were attempted with the JPL LN load, but the Styrofoam container developed a leak and had to be replaced by a smaller LN load assembly that had been developed previously by DSS-13 personnel for calibration purposes. The DSS-13 LN load absorbers were contained inside a cylindrical foam bucket with an inside diameter of 24.6 cm (9.7 in.). Six sets of differential system-temperature measurements with this DSS-13 LN load mounted above the X-/Ka-band dichroic plate resulted in a system-temperature decrease of 0.98 ± 0.15 K at 32 GHz.

The leak on the JPL LN load assembly was repaired by covering the inside bottom and inside walls of the foam bucket with a Kapton sheet (see Fig. 12). Tests were repeated on August 17, 1999, with the repaired larger JPL LN load installed, and test results showed that the system temperature was lowered 1.20 ± 0.10 K, which is 0.22-K lower than that obtained with the smaller DSS-13 LN load. As was expected, the large JPL LN load captured more of the stray Ka-band signals, and, hence, the improvement was more than that obtained with the DSS-13 LN load. It should be pointed out, however, that improvements obtained with either LN load were dramatic and significant.

Tests were not performed at X-band because, in order to capture stray X-band signals, a fabricated X-band LN load would have to be very large. There was not enough room to accommodate installation of a large X-band LN load.

G. Covered Panel Gaps

Another G/T improvement verification test that was performed involved putting 3.18-cm- (1.25-in.)-wide aluminum tape over all the gaps between antenna panels. Figure 14 shows an example of aluminum tape put over one of the antenna panel gaps. Figure 15 shows a partial view of the BWG antenna with all

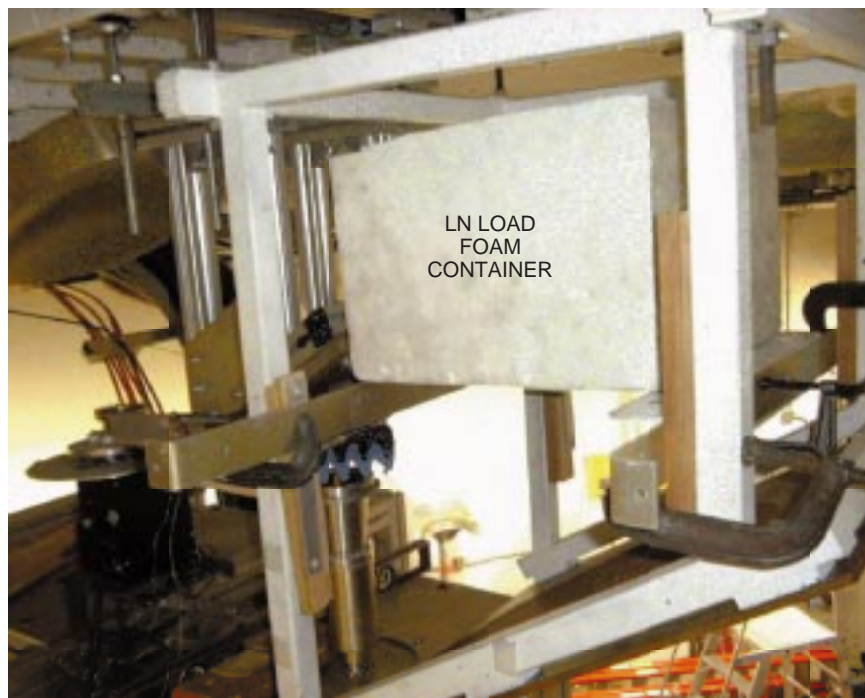


Fig. 13. Exterior view of the JPL-developed Ka-band liquid-nitrogen load installed above the X-band dichroic plate at DSS 13.



Fig. 14. Aluminum tape placed over a gap between antenna panels.



Fig. 15. Partial view of the DSS-13 BWG antenna main reflector after all panel gaps were covered with aluminum tape.

panel gaps covered with aluminum tape. On the first day of the test (August 17, 1999), aluminum tape was used to cover only those antenna-surface panel gaps that went in circumferential directions around the dish surface. The changes in T_{op} at both 8.420 and 32 GHz were measured before and after the aluminum tape covered only the circumferentially oriented panel gaps. On the second day of the test (August 19, 1999), aluminum tape was used to cover half the number of the radial gaps that ran from the BWG center to the edge of the dish surface. The changes in T_{op} at both 8.420 and 32 GHz again were measured before and after the tape was put on. The final test (performed on August 24, 1999) involved taping the remaining half of radial panel gaps on the DSS-13 BWG main-reflector surface.

It took approximately 2 hours to put new tape on the different panel gaps for each of the described test configurations. For these tests, the test procedure that was used to minimize baseline drifts was as follows. Just prior to making a configuration change, three successive mini-cals were performed. A mini-cal is a radiometer calibration sequence [4,5] that can be performed by striking the appropriate key on the computer keyboard. Then, immediately after the configuration change, three successive mini-cals again were performed. These mini-cals give T_{op} values that are corrected for radiometer gain changes. Then atmospheric noise temperatures, T_{atm} , that were measured by the advanced water vapor radiometer (AWVR) during the same test period were subtracted from the T_{op} values (corrected for gain changes) to give T_{op} minus T_{atm} values. Then these values were averaged for the appropriate test configurations. Remarkable repeatability and consistency of data were obtained using these measurement and data-reduction procedures.

The final data reductions, after making corrections for changes in gain and T_{atm} , showed that the system temperature due to taping all panel gaps was lowered by

$$0.31 \pm 0.05 \text{ K at } 8.425 \text{ GHz}$$

$$0.54 \pm 0.31 \text{ K at } 32 \text{ GHz}$$

where the tolerances are overall uncertainties that take into account uncertainties in the measurement results obtained on three different test configurations on three different dates. For comparison, the predicted improvement was 0.2 to 0.3 K for both X- and Ka-bands (see Table 1, Item 5)

III. Summary and Recommendations

Tests were performed only on those suggested improvement configurations shown in Table 1 that could be tested quickly and inexpensively. Table 7 gives comparisons of predicted and measured improvements. The total improvement was 1.2 ± 0.1 K at 8.420 GHz and 2.9 ± 0.4 K at 32 GHz. As shown in Table 3, an S-band degradation of 3.3 K was observed when the aperture plate had a 1.52-m- (5-ft)-diameter hole. If this degradation at S-band is acceptable, it is recommended that all the tested improvement configurations described in Table 7 be implemented. Otherwise, the aperture-plate configuration (Item 8) should not be implemented.

Table 7. Comparison of predicted and measured G/T improvements for the DSS-13 34-m BWG antenna.

Item	Suggestions for G/T improvement	Predicted X-/Ka-band improvement at 90-deg elevation angle	Measured improvement	
			X-band, K	Ka-band, K
1 ^a	Assemble skirts behind the subreflector (only three skirts at top of struts).	0.1–0.3 K	0.09 ± 0.05	0.13 ± 0.06
2 ^a	Cover hatch door opening.	0.03 K	Included in Item 3.	Included in Item 3.
3 ^a	Cover openings at base of struts.	0.1–0.2 K	0.08 ± 0.05	0.24 ± 0.09
4 ^a	Cover holography holes.	0.2–0.4 K	0.35 ± 0.05	0.5 ± 0.2
5 ^a	Close panel gaps.	0.2–0.3 K	0.31 ± 0.05	0.54 ± 0.31
6	Readjust panel using holography.	0.18 dB at Ka-band	—	—
7	Eliminate perforations using a solid panel.	0.2 K at X-band 0.4–0.7 K at Ka-band	—	—
8 ^a	Reduce the size of BWG opening hole near f1 [see Table 3, 1.52-m (5-ft) hole].	0.1–0.2 K	0.39 ± 0.03	0.29 ± 0.10
9	Close the gaps between mirrors and shroud.	0.1–0.3 K	—	—
10	Add skirt around the horn aperture.	0.1–0.2 K	—	—
11	Fabricate a new plug at the center of M5.	0.2–0.3 K	—	—
12 ^a	Install a flat cryo load behind a dichroic plate.	0.5–1.0 K	Not tested.	1.20 ± 0.10
Sum of measured improvements and rss of uncertainties.		—	1.2 ± 0.1	2.9 ± 0.4

^a Experimental verification tests were performed, and the results are reported in this article.

Acknowledgments

The authors are grateful to Juan Garnica of DSS 13, who designed and fabricated the aperture plate, and to Lester Smith of DSS 13, who designed the stand-off design that enabled mounting the aperture plate above the dish surface. The authors are grateful to personnel in the DSS-13 crew and to Jay Potter and Stan Hignett of the Modern Technology Corporation (MTC) Field Support Group at Goldstone for assisting in the installations of test configurations for most of the tests described in this article. DSS-13 personnel also performed most of the system-temperature measurements and assisted in the data reductions.

The authors are grateful for the assistance of Denny Wolff and Neil Buckman of the Planning Research Corporation (PRC), who obtained the aluminum dots and rolls of aluminum tape. Neil Buckman also designed the cone transition that was fabricated by the MTC Field Support Group at Goldstone. Steve Keihm of the Microwave and Lidar Technology Section provided advanced water vapor radiometer T_{atm} data for the panel gap tests and the nitrogen load tests.

References

- [1] D. A. Bathker, W. Veruttipong, T. Y. Otoshi, and P. W. Cramer, Jr., “Beam-Waveguide Antenna Performance Predictions with Comparisons to Experimental Results,” *Microwave Theory and Techniques*, Special Issue on Microwaves in Space, vol. MTT-40, no. 6, pp. 1274–1285, June 1992.
- [2] T. Y. Otoshi, “The Effect of Mismatched Components on Microwave Noise Temperature Calibrations,” *IEEE Transactions on Microwave Theory and Techniques*, Special Issue on Noise, vol. MTT-16, no. 9, pp. 675–686, September 1968.
- [3] T. Y. Otoshi, S. R. Stewart, and M. M. Franco, “A Portable X-Band Front-End Test Package for Beam-Waveguide Antenna Performance Evaluation, Part II: Tests on the Antenna,” *The Telecommunications and Data Acquisition Progress Report 42-105, January–March 1991*, Jet Propulsion Laboratory, Pasadena, California, pp. 54–68, May 15, 1991.
http://tmo.jpl.nasa.gov/tmo/progress_report/42-105/105G.PDF
- [4] T. Y. Otoshi, S. R. Stewart, and M. M. Franco, “A Portable X-Band Front-End Test Package for Beam-Waveguide Antenna Performance Evaluation, Part I: Design and Ground Tests,” *The Telecommunications and Data Acquisition Progress Report 42-103, July–September 1990*, Jet Propulsion Laboratory, Pasadena, California, pp. 135–150, November 15, 1990.
http://tmo.jpl.nasa.gov/tmo/progress_report/42-103/103N.PDF
- [5] C. T. Stelzried and M. J. Klein, “Precision DSN Radiometer Systems: Impact on Microwave Calibrations,” *Proceedings of the IEEE*, vol. 82, no. 5, pp. 777–789, May 1995. (For discussion of mini-cals, see the Appendix, p. 784.) Corrections in *Proceedings of the IEEE*, vol. 84, no. 8, p. 1187, August 1996.